Preprints, 12th IFAC Symposium on Dynamics and Control of Process Systems,
including Biosystems
Florianópolis - SC, Brazil, April 23-26, 2019

Detection and Estimation of Moving obstacles for a UAV

Thi Thoa Mac [*] **Cosmin Copot** [**] **Clara M. Ionescu** [***]

[*] *School of Mechanical Engineering, Hanoi University of Science and Technology, No.1 Dai Co Viet, Vietnam*
[**] *Department of Electromechanics, Op3Mech, University of Antwerp, Groenenborgerlaan 171, 2020 Antwerp, Belgium*
[***] *Dynamical Systems and Control Research Group, Department of Electrical Energy, Metals, Mechanical Constructions, and Systems, Ghent University, Ghent B-9052, Belgium.*

Abstract: In recent years, research interest in Unmanned Aerial Vehicles (UAVs) has been grown rapidly because of their potential use for a wide range of applications. In this paper, we proposed a vision-based detection and position/velocity estimation of moving obstacle for a UAV. The knowledge of a moving obstacle's state, i.e., position, velocity, is essential to achieve better performance for an intelligent UAV system specially in autonomous navigation and landing tasks. The novelties are: (1) the design and implementation of a localization method using sensor fusion methodology which fuses Inertial Measurement Unit (IMU) signals and *Pozyx* signals; (2) The development of detection and estimation of moving obstacles method based on on-board vision system. Experimental results validate the effectiveness of the proposed approach.

Keywords: UAV, obstacle detection, OpenCV, position/velocity estimation, autonomous navigation, sensor fusion.

1. INTRODUCTION

Recently, Unmanned Aerial Vehicles (UAVs) attract attentions both scholar and commercial interests within the autonomous vehicles community as the real and potential applications are numerous (F. Kendoul, (2012)).

Many studies of UAVs have emerged in the literature. Some examples of its application can be found in autonomous navigation of UAV in indoor environment (T. T. Mac et al., (2018)), traffic monitoring (K. Kanistras et al., (2015)), measurement and exploration in volcanic environments (C.D. Melita et al., (2015)), fire detection, monitoring, and extinguishing (L. Merino et al., (2015)), habitat mapping (N. Dijkshoorn, (2012)). Catching a falling object using a single UA, has been accomplished in (P. Bouffard, (2012)) and for a group of UAVs in cooperative formation in (R. Ritz et al., (2012)), where high-speed external cameras were applied to estimate the position of both the objects and UAVs.

In most applications, UAVs use Global Positioning System (GPS)/Inertial Navigation System to obtain the absolute positions, absolute velocities and attitude of the UAV in the working space. However, GPS signals can be disturbed easily, and cannot work when UAVs flying at low-altitude such as urban, mountain, forests or indoor environment (H. Chao et al., (2013)).

Other sensors used for UAV obstacle avoidance include multiple IR-UWB radars (Y. H. Shin et al., (2017)), cameras (J. A. G. Pulido et al., (2017)), Light Detection and Ranging (LIDAR) sensors (JS. Scherer et al., (2017)). In Y. H. Shin et al., (2017), the methods for detecting the ground (slope and roughness) and obstacles that based on the signals acquired by multiple impulse radio ultra-wide band are studied. An automatic expert system, based on image segmentation procedures that assists safe autonomous navigation through recognition and relative orientation of the UAV and platform, is proposed in (J. A. G. Pulido et al., (2017)). LIDAR sensors have been extensively investigated for safe area determination for small helicopters in (JS. Scherer et al., (2017)). Simultaneous localization and mapping (SLAM) is implemented to navigate UAV in working space (H. Alvarez et al., (2015)). In Mammarella et al., (2012); B. Herisse et al., (2012), an optical flow is used in the vision-based navigation approach. However, the UAV's position estimates cannot be obtained as optical flow can only measure the relative velocity of features. Consequently, the optical-flow-based navigation only works effectively in basic maneuvers, such as takeoff, landing, and hovering.

In J.W. Langelaan et al., (2007), a vision-based navigation system to enable a small UAV flight through a forest is presented when the trees positions are provided roughly by using a monocular camera and IMU. An unscented Kalman Filter (UKF) is applied to estimate the UAV's states and the trees positions in the forest. Simulation results for an UAV navigating through a 2D environment

[⋆] Coresspoding author: Thi Thoa Mac (e-mail: thoa.macthi@hust.edu.vn).

are implemented. However, the initial states of the UAV (position and velocity) are assumed to be known in advance. In L. Huang et al., (2017), the vision inertial absolute navigation system (VIANS) for an UAV using landmarks is developed. Firstly, the model of the VIANS is implemented. Secondly, Extend Kalman Filter (EKF) and Unscented Kalman Filter (UKF) are applied, respectively, to estimate the absolute position, absolute velocity and attitude of the UAV. Lastly, the influence of landmark distribution on observability, convergence speed and estimation accuracy of the VIANS are validated through simulations.

Current implementations of a UAV still require a robust autonomous navigation algorithm in dynamic environments. Therefore, the knowledge of a moving obstacle's state, i.e., position, velocity, is a crucial issue to achieve realizable performance from most UAV intelligent systems. Several dynamic position and velocity estimation algorithms have been proposed. It is possible with a system based on vision or GPS (J. Cobano et al., (2008); S. H. Liu et al., (2010)). In G. Farneback, (2010), a velocity estimation algorithm which uses orientation tensors and parametric motion models, is developed to provide accurate results however the speed is somewhat slow.

In this paper, a proposed vision-based detection and estimation approach of moving obstacle for a UAV autonomous navigation is presented. This work is an initial step for the development of fully autonomous navigation and landing of a UAV in dynamic environment. The main contributions of this research are: (i) the development of a position-estimation approach using sensor fusion methodology which fuses IMU signals and *Pozyx* signals; (ii) the design and implementation of a vision-based detection and estimation of moving obstacles for a UAV autonomous navigation.

The paper is organized as follows. A brief description of the Ar.Drone 2.0 platform used in this study is introduced in section 2. System setup and localization method are presented in section 3. Obstacle detection and estimation are described in section 4. The experimental results are provided in section 5. Finally, section 6 includes conclusions and suggestions for further work.

2. AR.DRONE 2.0 QUADROTOR PLATFORM

An Ar.Drone 2.0, a commercial and low-cost micro UAV, is used in this work. This drone includes four propeller blades arranged symmetrically around a central unit which includes the sensory equipment and the circuit board. There are four basic motions of this quadrotor: pitch, roll, throttle and yaw as shown in Fig. 1.

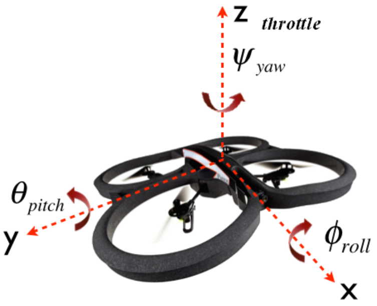

Fig. 1. The movements of an AR.Drone 2.0.

The sensor system of this drone consists of several motion sensors which together form an IMU. The communication between an Ar.Drone and a command station is performed via Wi-Fi connection within a 50 meters range. The Ar.Drone 2.0 is equipped with two cameras, one in the bottom part and the other in frontal part. They have resolutions of 320 x 240 pixels at 30 frames per second (fps) and 640 x 360 pixels at 60 fps, respectively.

Several Software Development Kits (SDK) have been developed for Windows, Linux or iOS operating systems S. Piskorski et al., (2012); T. Krajnik et al., (2011); (2013), thus enabling the AR.Drone 2.0 to be manipulated from a computer, smart phone or tablet. In this study, the Ar.Drone 2.0 is controlled from a computer using Visual Studio C++, OpenCV and cvdrone.

The developed SDK mode allows the drone to transmit and receive the information of roll angle (rad), pitch angle (rad), the altitude (m), yaw angle (rad) and the linear velocities on longitudinal/ transversal axes (m/s). They are denoted by $\{\theta_{out},\ \phi_{out},\ \zeta_{out},\ \psi_{out},\ \dot{x},\ \dot{y}\}$ respectively. The system is executed by four inputs $\{V_{in}^{x},\ V_{in}^{y},\ \dot{\zeta}_{in},\ \dot{\psi}_{in}\}$ which are the linear velocities on longitudinal/transversal axes, vertical speed and yaw angular speed references as depicted in Fig. 2. The control parameters given to the internal controllers are floating point values between [-1, 1]. Those parameters are not directly the control parameters values, but a percentage of the maximum corresponding values of the mentioned controller.

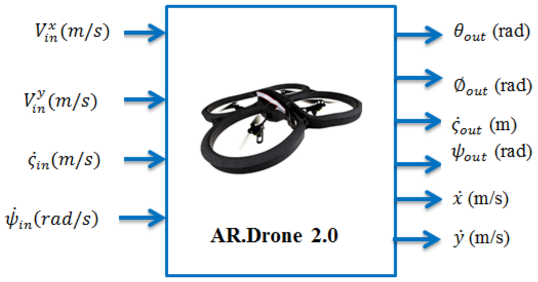

Fig. 2. Inputs and Outputs of a AR.Drone 2.0.

3. SETUP SYSTEM AND LOCALIZATION

The setup consists of a Lego Mindstorm that is driving with a constant speed of 0.2 m/s and a hovering drone that estimates the velocity of the bot using its bottom camera as shown in Fig. 3.

The system setup and the proposed localization based on sensor fusion are developed in a lab-scale environment. For real-life application outdoors, wind gust and other issues may arise, which are not discussed here.

In order to perform autonomous assignments, an accurate position estimation is essential requirement. In outdoor applications, GPS usually provides an estimation that is accurate enough however, it is not an effective tool for indoor applications. There are several options for indoor

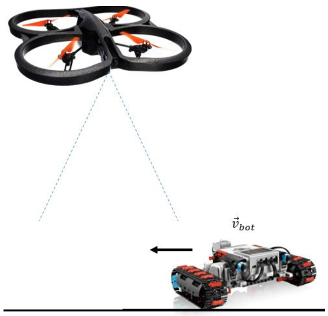

Fig. 3. The setup system.

position estimation such as: visual navigation, the onboard IMU data or extra sensors. This section is concerned with the state estimation of an UAV in indoor environment using sensor fusion which fuses IMU signals and *Pozyx* signals.

The IMU measures the roll, pitch and yaw angle of the UAV. The velocity estimations are obtained by fusing the information from a 3-axis gyroscope with the information from a 3-axis accelerometer and a magnetometer. Position estimations can then be obtained by integrating the velocities. As the velocities are given in drone coordinates, a coordinate transformation to real world coordinates is required.

$$x_k = x_{k-1} + \begin{bmatrix} \cos(yaw) & -\sin(yaw) & 0 \\ \sin(yaw) & \cos(yaw) & 0 \\ 0 & 0 & 1 \end{bmatrix} \cdot V_{drone} \cdot \Delta t \quad (1)$$

where:
V_{drone} is velocity of the drone;
x_k, x_{k-1} are position of the drone in x direction at sample k, $k-1$;
Δt is sample time.
The y position is calculated in the similar approach. The better estimation of the height can be obtained by fusing the velocity in z-direction with the information from the ultrasonic sensor.

To use *Pozyx* for the localization of a Ar.Drone 2.0, the position estimation is implemented by using ultra-wide band technology. The position estimation accuracy of this equipment is ±10 cm. Please refer to software, (2013). Three anchors are placed in a room (see Fig. 4). The anchors should not be placed on one line or on one plane. The absolute position of these anchors needs to be known in advance. By measuring the distance between the *Pozyx* tag and each anchor, the position of the *Pozyx* (UAV position) tag can be estimated. These were filtered out by defining a maximum allowed deviation of the current position compared to the previous one. When the deviation exceeds the threshold value, the current position is set equal to the previous one. The *Pozyx* offers a robust position estimation. The results obtained by unfiltered and filtered *Pozyx* is shown in Fig. 5.

To combine the advantage of the IMU and the *Pozyx*, we fused these signals. A Kalman filter is used to combine the information of different sensors. The state of the UAV is $(x, y, z, v_x, v_y, v_z)^T$.

A Kalman filter consists of two phases: the prediction phase and the update phase. In the prediction phase, the Kalman filter estimates the position and its uncertainty based on the physical model.

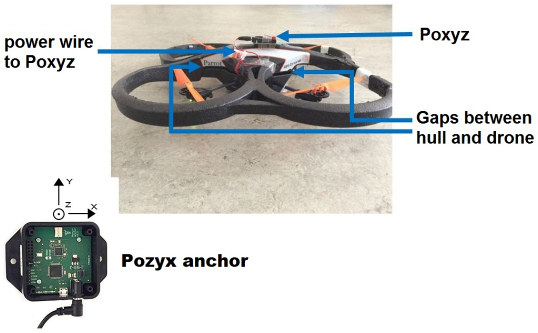

Fig. 4. The Ar.Drone 2.0 equipped Pozyx and its anchor.

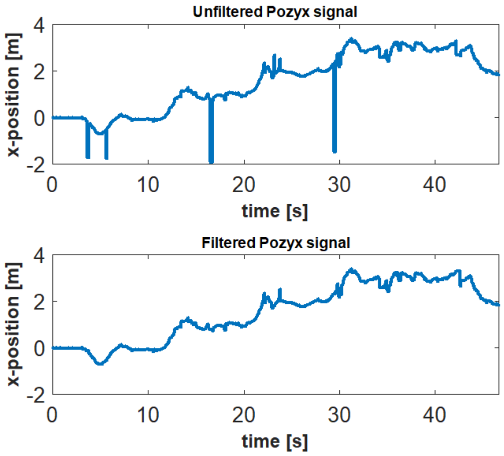

Fig. 5. Unfiltered compared to Filtered Poxyz signal.

$$\hat{x}_k = A \cdot \hat{x}_{k-1} \quad (2)$$

$$P_k = A \cdot P'_{k-1} \cdot A^T + Q \quad (3)$$

In the update phase the observed measurements are used to find a new best estimate.

$$K' = P_k \cdot C^T (C \cdot P_k \cdot C^T + R)^{-1} \quad (4)$$

$$\hat{x}'_k = \hat{x}_k + K'(z_k - C \cdot \hat{x}_k) \quad (5)$$

$$P'_k = P_k - K' \cdot C \cdot P_k \quad (6)$$

The transition matrix A was chosen as in (7). The variable dt is equal to the mean execution time of the loop. With the used sensors, it is possible to measure the state directly, so the measurement matrix C is equal to an unity matrix.

$$A = \begin{bmatrix} 1 & 0 & 0 & dt & 0 & 0 \\ 0 & 1 & 0 & 0 & dt & 0 \\ 0 & 0 & 1 & 0 & 0 & dt \\ 0 & 0 & 0 & 1 & 0 & 0 \\ 0 & 0 & 0 & 0 & 1 & 0 \\ 0 & 0 & 0 & 0 & 0 & 1 \end{bmatrix} \quad (7)$$

$$C = \begin{bmatrix} 1 & 0 & 0 & 0 & 0 & 0 \\ 0 & 1 & 0 & 0 & 0 & 0 \\ 0 & 0 & 1 & 0 & 0 & 0 \\ 0 & 0 & 0 & 1 & 0 & 0 \\ 0 & 0 & 0 & 0 & 1 & 0 \\ 0 & 0 & 0 & 0 & 0 & 1 \end{bmatrix} \quad (8)$$

To design a Kalman filter, the process noise covariance Q and the measurement noise covariance R are added. The covariances of the *Pozyx* were then tuned manually until the desired result was obtained.

$$Q = \begin{bmatrix} 0.1 & 0 & 0 & 0 & 0 & 0 \\ 0 & 0.1 & 0 & 0 & 0 & 0 \\ 0 & 0 & 0.1 & 0 & 0 & 0 \\ 0 & 0 & 0 & 0.3 & 0 & 0 \\ 0 & 0 & 0 & 0 & 0.3 & 0 \\ 0 & 0 & 0 & 0 & 0 & 0.3 \end{bmatrix} \tag{9}$$

$$R = \begin{bmatrix} 10 & 0 & 0 & 0 & 0 & 0 \\ 0 & 10 & 0 & 0 & 0 & 0 \\ 0 & 0 & 10 & 0 & 0 & 0 \\ 0 & 0 & 0 & 0.05 & 0 & 0 \\ 0 & 0 & 0 & 0 & 0.05 & 0 \\ 0 & 0 & 0 & 0 & 0 & 0.05 \end{bmatrix} \tag{10}$$

Fig. 6 illustrates an estimation of the position with sensor fusion, *Pozyx* and IMU only. In the experiment, the UAV starts at $x \approx 0\ m$, then goes around 21 seconds to $x \approx 1\ m$ and finally goes around 30 seconds to $x \approx 2\ m$. It is obvious to not only use the IMU for position estimation as it starts to drift very quickly. The *Pozyx* has a robust position estimation but it is noisy. The sensor fusion combines the advantages of both signals. It provides a robust estimation without noise.

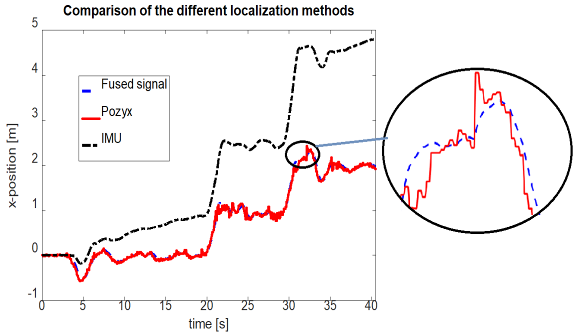

Fig. 6. Comparison of the different localization methods.

4. VISION BASED OBSTACLE DETECTION

To recognize unknown moving obstacles, advanced sensors are needed instead of the ones that are currently installed on the Parrot Ar.Drone 2.0. It is not possible to install extra sensors due to weight restrictions. That is why the moving obstacles are marked so that they can be detected with the bottom camera. To show the concept, the moving obstacles are marked with colored paper. The obstacles are then filtered based on their color. From this, the position of the obstacles can be determined.

4.1 Obstacle detection and estimation

To be able to detect the position of the colored paper, each pixel that has a certain HSV value should be converted to a binary value that indicates if the obstacle (colored paper) is present in that pixel. To perform this conversion, a range of hue, saturation and value needs to be specified that corresponds to the colored paper. To obtain a rectangle that includes the object as shown in Fig. 7, the standard contour tracing function of OpenCV is used.

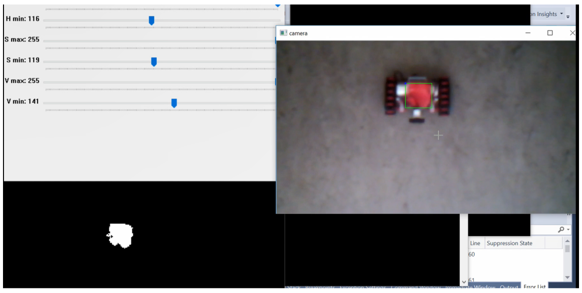
H min: 116
S max: 255
S min: 119
V max: 255
V min: 141

Fig. 7. Color based tracking moving obstacle.

4.2 Conversion coordinates

It is possible to extract the pixel coordinates of the obstacle based on the contour detection process. These coordinates are converted to the real-world coordinates to have an estimation of the position and the velocity of the obstacle. The calculation is implemented based on the diagram as shown in Fig. 8. In which M is center point of the received image. P is the position of the Lego robot in the image coordinates. AOV_x is the angle of field of view and D presents bottom camera of the AR.Drone 2.0. O is projection point of D in horizontal plane. W is intersection point between DP and horizontal plane. The following formulas are applied. $|PM|$ presents $|X_P - X_M|$

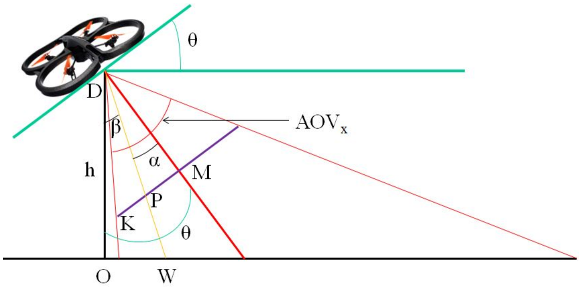

Fig. 8. Conversion from point in pixel coordinates to real-world coordinates in $1D$

with X_M is the x-coordinate of the M-the middle point of the picture and X_P the x-coordinate of P.

$$|DM| = \frac{|KM|}{\tan(AOV_x/2)} \tag{11}$$

$$\alpha = \arctan(\frac{|PM|}{|DM|}) \tag{12}$$

β presents $\theta \pm \alpha$, the sign depends whether $X_P > X_M$ or $X_P < X_M$ therefore α' is introduced.

$$\alpha' = \arctan(\frac{X_P - X_M}{|DM|}) \tag{13}$$

We have:

$$\beta = \theta + \alpha' \tag{14}$$

From which the x-coordinate in drone coordinates (with respect to the drone) results:

$$x_W = \tan(\beta) \cdot h \tag{15}$$

with $DO = h$

The absolute world x-coordinate of the object is then:

$$x_{obj} = x_{drone} + \cos(yaw) \cdot x_W - \sin(yaw) \cdot y_W \quad (16)$$

In the similar approach, the y-coordinate of the object (moving obstacle) is:

$$y_{obj} = y_{drone} + \cos(yaw) \cdot y_W + \sin(yaw) \cdot x_W \quad (17)$$

5. EXPERIMENT RESULTS

For safe autonomous navigation/landing in presence of moving obstacle, an essential requirement is perception of the position and velocity of the moving object. To validate our approach, the system setup consists of a Lego Mindstorm that is driving with a constant speed of 0.2 m/s and an Ar.Drone 2.0 that estimates the velocity of the robot using its bottom camera.

5.1 Position estimation of the moving obstacle

This subsection presents the results of position estimation of the moving obstacle using bottom camera of the drone. In Fig. 9, Fig. 10, the position of the drone, the position of the robot with respect to the drone and the (absolute) position of the robot are obtained. When the estimations are equal to zero, the robot is not in sight of the drone. The x-position is linearly dependent of time which corresponds to a constant velocity. The y-position fluctuates between zero and 0.1 m, which indicates that the real deviation of the y-position is low. The fluctuations are mainly caused by the imperfect localization of the drone, the delay between localization of the drone and the position estimation of the robot by camera and the fact that samples are taken in discrete intervals. These shortcomings mainly affect the estimation when the drone is very dynamic.

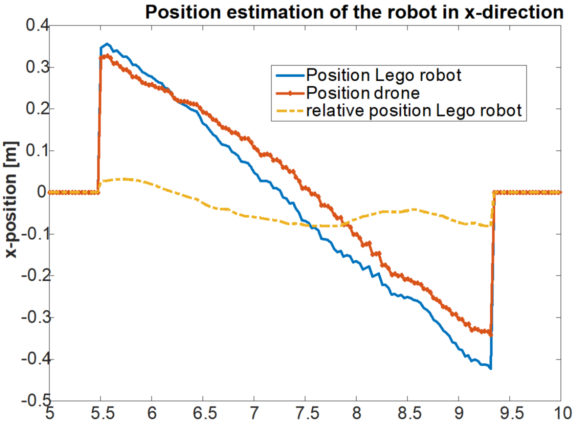

Fig. 9. Position estimation of the robot in x-direction.

5.2 Velocity estimation

To obtain a proper velocity estimation, a cumulative moving average filter is applied in this application. This result shows that the measurement is reasonable at the first stage (at 1.5 first seconds) as shown in Fig. 11. Thereafter, the velocity estimation is quite accurate as shown in Fig. 12. The experiment shows that velocity estimations based on vision system is feasible from a drone. Even considering delays, accurate velocity estimations of moving obstacles are obtained.

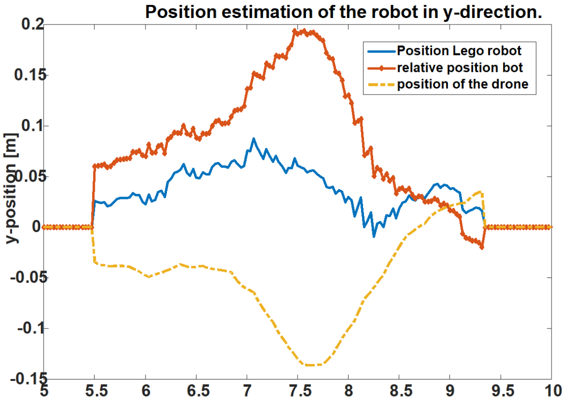

Fig. 10. Position estimation of the robot in y-direction.

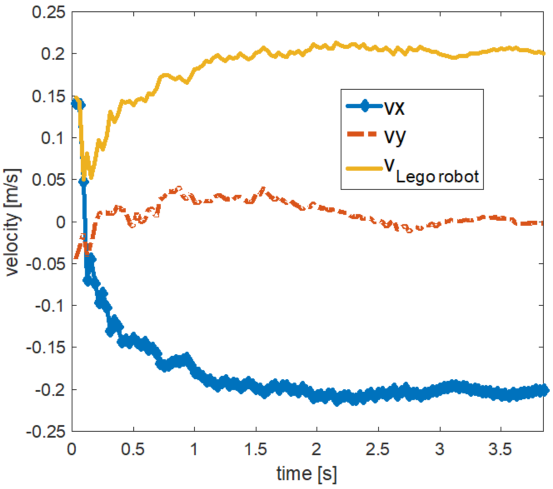

Fig. 11. Moving average filter that is applied on the velocity measurements of the moving obstacle.

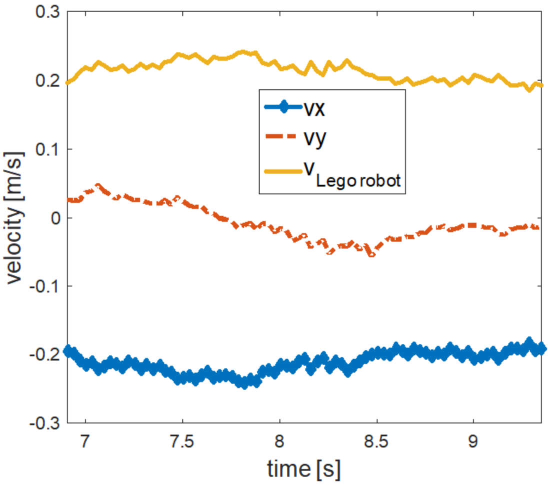

Fig. 12. Cumulative moving average filter that is applied on the velocity measurements of the moving obstacle after 1.5s.

6. CONCLUSION

This paper proposed a vision-based detection and estimation moving obstacles of a commercial AR. Drone 2.0.

The system is described from electromechanical point of view. The knowledge of a moving obstacle's state, i.e., position, velocity, assists the UAV navigate automatically in working environment. The main contributions include (i) The development of a localization methodology using sensor fusion technique which fuses IMU signals and *Pozyx* signals; (ii) Design and implementation an effective estimation of moving obstacle's position and velocity based on on-board vision system. The results indicate that the obtained model fits properly to the measured data. The designed strategy is able to detect and estimate accurately the state of the dynamic obstacle. This research is the first step to develop autonomous navigation and landing of the UAV in a dynamic environment. Future work includes implementation the algorithm with multiple moving obstacles with different speeds and multiple UAVs.

ACKNOWLEDGEMENTS

Mac Thi Thoa is funded by the National Foundation for Science and Technology Development of Vietnam NAFOSTED. The authors would like to gratefully thank Arne Maenhaut for his assistance in conducting the experiments.

REFERENCES

F. Kendoul (2012), Survey of advances in guidance, navigation, and control of unmanned rotorcraft systems, *Journal of Field Robotics, vol. 29 (2), pp. 315-378.*

T. T. Mac, C. Copot, R. De Keyser, M. Ionescu (2018), The Development of an Autonomous Navigation System with Optimal Control of an UAV in Partly Unknown Indoor Environment, *Mechatronics, vol. 49, pp. 187-196.*

K. Kanistras, G. Martins, M.J. Rutherford, K.P. Valavanis (2015), Survey of Unmanned Aerial Vehicles (UAVs) for Traffic Monitoring, *Handbook of Unmanned Aerial Vehicles, Springer, Dordrecht, pp. 2643-2666*

C.D. Melita, D. Longo, G. Muscato, G. Giudice (2015), Measurement and Exploration in Volcanic Environments, *Handbook of Unmanned Aerial Vehicles, Springer, Dordrecht, pp. 2667-2692*

L. Merino, J.R. Martinez-de Dios, A. Ollero (2015), Cooperative Unmanned Aerial Systems for Fire Detection, Monitoring, and Extinguishing, *Handbook of Unmanned Aerial Vehicles, Springer, Dordrecht, pp. 2693-2722*

N. Dijkshoorn (2012), Simultaneous localization and mapping with the AR.Drone, *Master's thesis, University of Amsterdam*

P. Bouffard (2012), On-board Model Predictive Control of a Quadrotor Helicopter: Design, Implementation, an Experiments, *Master's thesis, University of California, Berkeley, CA, USA*

R. Ritz, M. Muller, M. Hehn, R. Dandrea (2012), Cooperative quadrocopter ball throwing and catching, *In Proceedings of the IEEE/RSJ International Conference on Intelligent Robots and Systems (IROS), Algarve, Portugal, pp. 4972-4978*

H. Chao, Y. Gu, J. Gross, G. Guo, M.L. Fravolini, and M.R. Napolitano (2013), A Comparative Study of Optical Flow and Traditional Sensors in UAV Navigation, *American Control Conference, Washington, DC, USA, pp. 3859-3863*

Y. H. Shin, S. Lee, J. Seo (2017), Autonomous safe landing-area determination for rotorcraft UAVs using multiple IR-UWB radars, *Aerospace Science and Technology, Vol. 69, pp. 617-624*

J. A. G. Pulido, G. Pajares, S. Dormido, J.M. De la Cruz (2017), Recognition of a landing platform for unmanned aerial vehicles by using computer vision-based techniques *Expert Systems with Applications, vol. 76, pp. 152-165*

S. Scherer, L. Chamberlain, S. Singh (2012), Autonomous landing at unprepared sites by a full-scale helicopter *Robotics and Autonomous Systems, vol. 60(12), pp. 1545-1562*

H. Alvarez, L. M. Paz, J. Sturm, D. Cremers (2015), Collision Avoidance for Quadrotors with a Monocular Camera *Experimental Robotics, Vol. 109, Springer Transactions in Advanced Robotics pp. 195-209*

M. Mammarella, G. Campa, M.L. Fravolini (2012), Comparing optical flow algorithms using 6-DOF motion of real-World rigid Objects *IEEE transactions systems man cybernetics, Part C, vol.42 (6), pp. 1752-1762*

B. Herisse, T. Hamel, R. Mahony (2012), Landing a VTOL unmanned aerial vehicle on a moving platform using optical flow *IEEE Transaction on Robotics, vol. 28(1), pp. 77-89*

J.W. Langelaan (2007), State estimation for autonomous flight in cluttered environments *Guidance Control Dynamic, vol. 30 (5), pp. 1414-1426*

L. Huang, J. Song, C. Zhang (2017), Observability analysis and filter design for a vision inertial absolute navigation system for UAV using landmarks, *Optik, vol. 149, pp. 455-468*

L. Huang, J. Song, C. Zhang (2008), Location of legged robots in outdoor environments *Robotics and Autonomous Systems, vol. 56, no. 9, pp. 751–761*

S. H. Liu, T. S. Huang, and J. Y. Yen (2010), Comparison of sensor fusion methods for an sma-based hexapod biomimetic robot *Robotics and Autonomous Systems, vol. 58, no. 5, pp. 737–744*

G. Farneback (2010), Very High Accuracy Velocity Estimation using Orientation Tensors, Parametric Motion, and Simultaneous Segmentation of the Motion Field, *IEEE International Conference on Computer Vision, pp. 171–177*

S. Piskorski, N. Brulez, E. Eline, F. D Haeyer (2012), *Ar. drone developer guide-sdk 2.0*

T. Krajnik, V. Vonasek, D. Fiser, and J. Faigl (2011), Ar.drone as a platform for robotic research and education, *Research and Education in Robotics - Eurobot, Volume 161, pp.172-186*

https://github.com/puku0x, cv drone free software, December 2013.

https://www.pozyx.io/